

This is an Open Access document downloaded from ORCA, Cardiff University's institutional repository:<https://orca.cardiff.ac.uk/id/eprint/123433/>

This is the author's version of a work that was submitted to / accepted for publication.

Citation for final published version:

Nuzzo, Stefano, van Leusen, Jan, Twamley, Brendan, Platts, James A. , Kögerler, Paul and Baker, Robert J. 2019. Oxidation of uranium(IV) thiocyanate complexes: cation–cation interactions in mixed-valent uranium coordination chains. *Dalton Transactions* 48 (20) , pp. 6704-6708. 10.1039/C9DT01005J

Publishers page: <http://dx.doi.org/10.1039/C9DT01005J>

Please note:

Changes made as a result of publishing processes such as copy-editing, formatting and page numbers may not be reflected in this version. For the definitive version of this publication, please refer to the published source. You are advised to consult the publisher's version if you wish to cite this paper.

This version is being made available in accordance with publisher policies. See <http://orca.cf.ac.uk/policies.html> for usage policies. Copyright and moral rights for publications made available in ORCA are retained by the copyright holders.



Oxidation of uranium(IV) thiocyanate complexes: cation–cation interactions in mixed-valent uranium coordination chains†

Stefano Nuzzo,^a Jan van Leusen,^b Brendan Twamley,^a James A. Platts,^c Paul Kögerler^b and Robert J. Baker^{*a}

Oxidation of $\text{Cs}_4[\text{U}(\text{NCS})_8]$ in MeCN or DMF affords structurally characterised examples of the mixed-valent $\text{U}^{\text{IV/VI}}$ compound $\text{Cs}_{14}\{\{\text{U}(\text{NCS})_8\}_3\{\text{UO}_2(\text{NCS})_4(\text{H}_2\text{O})\}\}\cdot 4.5\text{H}_2\text{O}$, or the $[\text{U}^{\text{IV}}-\text{U}^{\text{V}}-\text{U}^{\text{IV}}][\text{U}^{\text{VI}}]$ species $[\text{U}(\text{DMF})_8(\mu\text{-O})\text{U}(\text{NCS})_5(\mu\text{-O})\text{U}(\text{DMF})_7(\text{NCS})][\text{UO}_2(\text{NCS})_5]$. Vibrational and magnetism data support their oxidation state formalism, which is further corroborated by computational methodology.

Actinide chemistry has undergone a significant expansion of interest in recent years¹ and new characterisation techniques have augmented impressive and innovative synthetic protocols. An understanding of how 5f and 6d orbitals participate in bonding to enhance covalency in metal–ligand overlap is emerging. Striking examples include the discovery of a new oxidation state $\text{U}(\text{II})$ whose electronic structure depends on the ligands.² The chemistry of uranium, which does not require the use of specialised facilities, has been at the forefront of this revolution and fundamentally new organometallic and coordination chemistry examples are replete in the current literature.^{1a,d} One area where understanding is still limited is the magnetic behaviour of actinides, and uranium compounds are at the cutting edge.³ For example, 5f U^{III} compounds have repeatedly been shown to exhibit unusual magnetization dynamics and are candidates for single-molecule and single-ion magnets.^{3b–d} 5f U^{V} compounds also have anisotropy and can show similar magnetic behaviour, on its own⁴ or in combination with transition metals⁵ or lanthanides.⁶ These mixed-metal complexes are typically assembled via cation–cation interactions (CCI). This involves interactions of the $[\text{UO}_2]^+$ ion

with another metal ion via a UVO_y interaction, i.e. the $-y$ oxygen acting as a Lewis base.⁷ This interaction between actinyl units is rather rare, but gaining in significance and a likely method for the disproportionation⁸ reaction of $[\text{UO}_2]^+$. The manifestations of CCIs on the magnetochemical properties are fundamental to our understanding of the magnetic coupling mechanisms, as an a priori prediction for SMM behaviour of actinide ions is not currently possible.

We have an interest in thorium(IV) and uranium(IV) thiocyanate complexes as a platform to study how photo-luminescence spectroscopy can delineate oxidation states.⁹ We have recently shown that the π -donor ability of the $[\text{NCS}]^-$ ion does not stabilise the U^{III} oxidation state;¹⁰ in the solid state, $[\text{U}(\text{NCS})_8]^{4-}$ ions are stable in air for months but they undergo slow oxidation in solution. Herein we report on a structural study of the air oxidation of $\text{Cs}_4[\text{U}(\text{NCS})_8]$ in MeCN (1) and DMF (2) and an investigation of the photophysical and magnetic (2) properties. Crystallisation of $\text{Cs}_4[\text{U}(\text{NCS})_8]$ from MeCN over one month formed emerald green crystals of 1 showing vibrational bands assigned as $\nu_1(\text{U}^{\text{VI}}\text{VO}) = 844 \text{ cm}^{-1}$ and $\nu_3(\text{U}^{\text{VI}}\text{VO}) = 922 \text{ cm}^{-1}$. When this recrystallisation was

repeated in DMF, dark green crystals of 2 were deposited. Bands typical for $\nu_1(\text{U}^{\text{VI}}\text{VO}) = 846 \text{ cm}^{-1}$ and $\nu_3(\text{U}^{\text{VI}}\text{VO}) = 912 \text{ cm}^{-1}$ are observed, along with those more characteristic of $[\text{UO}_2]^+$ at $\nu_1(\text{U}^{\text{V}}\text{VO}) = 815 \text{ cm}^{-1}$ and $\nu_3(\text{U}^{\text{V}}\text{VO}) = 865 \text{ cm}^{-1}$.^{5,6} The calculated force constants k_1 and k_{12} show the expected weaker bond in the U^{V} vs. U^{VI} in 2 (Fig. S1 and S2; Table S3†). UV-vis/NIR spectroscopy revealed f–f transitions typical of U^{IV} in both 1 and 2 (Fig. S3–S6†); bands for $[\text{UO}_2]^+$ are generally weak and obscured by U^{IV} . These data point to a mixed oxidation state species. If crystals of 1 or 2 are redissolved in MeCN and stored in the air for a month, the colour changes to yellow and single crystals are deposited upon vapour diffusion with $^i\text{Pr}_2\text{O}$; the structure shows them to be $\text{Cs}_3[\text{UO}_2(\text{NCS})_5]$.^{9c}

The nature of 1 and 2 have been confirmed by single-crystal X-ray diffraction: 1 is of the composition $\text{Cs}_{14}\{\{\text{U}(\text{NCS})_8\}_3\{\text{UO}_2(\text{NCS})_4(\text{H}_2\text{O})\}\}\cdot 4.5\text{H}_2\text{O}$ (Fig. 1, S7 and 8†), and 2, $[\text{U}(\text{DMF})_8(\mu\text{-O})\text{U}(\text{NCS})_5(\mu\text{-O})\text{U}(\text{DMF})_7(\text{NCS})][\text{UO}_2(\text{NCS})_5]$

^aSchool of Chemistry, University of Dublin, Trinity College, Dublin 2, Ireland. E-mail: bakerrj@tcd.ie

^bInstitute of Inorganic Chemistry, RWTH Aachen University, D-52074 Aachen, Germany

^cSchool of Chemistry, Cardiff University, Park Place, Cardiff, CF10 3AT, UK

†Electronic supplementary information (ESI) available: Further spectroscopic data and details of calculations and magnetism. CCDC 1851382–1851383. For ESI and crystallographic data in CIF or other electronic format see DOI: 10.1039/c9dt01005j

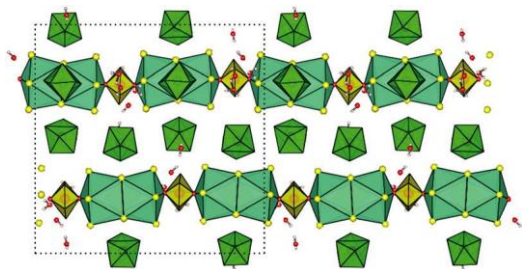


Fig. 1 Partial structure of 1 along the crystallographic *c*-axis showing the CCI between the uranyl (yellow polyhedra) and Cs (blue polyhedra); S = yellow, O = red, green polyhedra = U(IV).

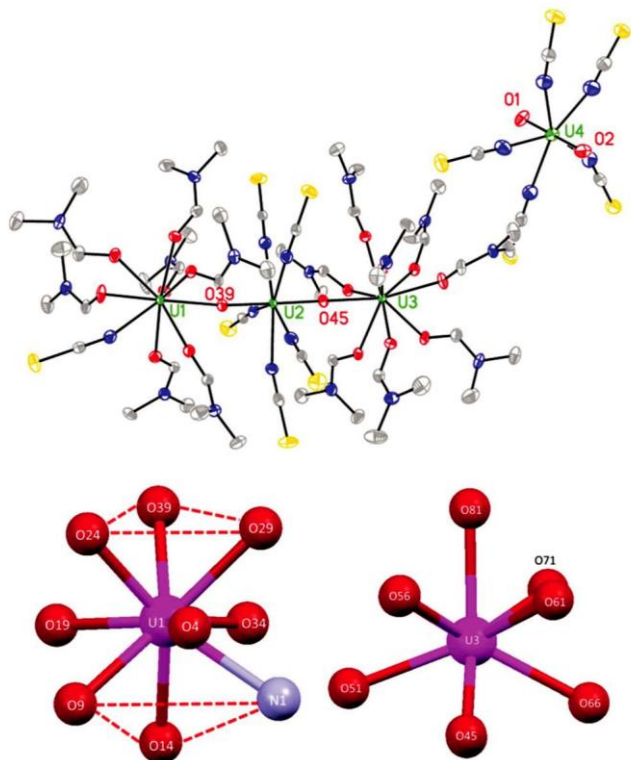


Fig. 2 Top: Asymmetric unit of 2. Hydrogen atoms omitted and only U and selected heteroatoms labelled for clarity; bottom: coordination geometry around U1 and U3.

(Fig. 2). In 1 and 2, the NvC and CvS bonds are invariant irrespective of oxidation state, consistent with our previous studies on U^{IV} and U^{VI} thiocyanate complexes.^{9,11} Compound 1 crystallises as a coordination polymer containing three U^{IV} and a U^{VI} ion, with average U^{VI}-N (2.400 Å), U^{IV}-N (2.433 Å), and U^{VI}vO (1.770(7) and 1.777(6) Å) bond lengths in line with our previous examples.^{9,11} Each U^{IV} ion adopts a square antiprismatic coordination environment. However, the most interesting structural feature is the CCI between the -yl and Cs⁺ ion (O-Cs: 2.974(2) Å) that bridges to a second Cs ion through Cs-S-Cs interactions (Fig. 1). The water molecule coordinated to the uranyl ion hydrogen bonds to the water coordinated to the Cs⁺ ion (O...O: 2.726(13) Å).

In order to assign oxidation states in 2, bond valence sum analysis¹² gives 4.35 (U1), 4.79 (U2), 4.47 (U3), and 5.61 (U4), indicating a charged-balanced [U^{IV}-U^V-U^{IV}][U^{VI}] system. In 2, the average U^{VI}-N (2.460 Å), U^V-N (2.458 Å) and U^{IV}-N (2.471(6) Å) follow the expected trend based on ionic radii,¹³ but are longer than in 1. The U^{VI}vO bond lengths (1.783(6) and 1.769(6) Å) are typical¹¹ and the U^VvO bonds at 1.915(5) and 1.922(5) Å, more characteristic for uranyl(v) ions engaged in CCI, and not a U^{IV}-O-U^{IV} arrangement as these bond lengths are longer at 2.058(3) Å in the complex [(UO₂I₄){U(i)Cl(py)₄}₂].^{6b} The U^{IV}-ODMF bond lengths range from 2.379(5) to 2.474(5) Å and the -yl oxygen involved in the CCI shorter at U(1)-O(39) = 2.311(5) Å and U(3)-O(45) = 2.299(5) Å, with a linear OvUvO fragment (O(39)-U(2)-O(45) = 178.9(2)°). U1 adopts a distorted tricapped trigonal prism environment (as described by continuous shape measures, Table S2†).¹⁴ Closer inspection of the bond lengths and angles confirm this: the longer U-ODMF bonds are associated with the capping ligands (U(1)-O(4) = 2.474(5) Å; U(1)-O(19) = 2.472(5) Å; U(1)-O(34) = 2.440(5) Å) and the O-U-O angles are 114°, 117° and 128°. The O-U-O angles in the trigonal prism are 70–80°. The geometry around U3 is a mono-capped square antiprism, where O81 is the capping oxygen and has the longest bond length (2.461(5) Å). It is instructive to compare the U(3)-O bond lengths to that of [U(DMF)₉]ⁿ⁺ (n = 3,¹⁵ 4)¹⁶ which has the same geometry: the U-O bonds that define the square antiprism are 2.52(3) Å for U^{III} and 2.37(1) Å for U^{IV}; in 2 these bond lengths average at 2.39(5) Å corroborating the assignment of U^{IV}. In contrast to our previous structural analysis¹¹ of [R₄N][UO₂(NCS)₅], there are no significant C-H...S or C-H...O hydrogen bonds.

2 is amenable to a thorough photophysical examination as all three oxidation states have been reported to be emissive.¹⁷ The [UO₂]²⁺ ion has extensive and well understood emission profiles whilst if U^{IV} compounds do not have ligand-based charge transfer bands in the visible region then rather weak bands with a short lifetime are observable.⁹ [UO₂]⁺ ions have been reported to be emissive, though these reports are sparse.¹⁸ The emission spectra of single crystals of 2 dissolved in MeCN (ca. 10⁻⁶ M) show two very broad, uninformative features (Fig. S12†). Solid state emission spectra of powdered single crystals at 77 K are more revealing and show bands between 350 nm and 480 nm and U^{VI} from 490–580 nm (Fig. 3). The vibronic coupling and peak positions of the uranyl bands are identical to that reported for [R₄N]₃[UO₂(NCS)₅],¹¹ whilst the U^{IV} component is consistent with [Li(THF)₄][UCl₅(THF)]^{9a} or [Et₄N]₄[U(NCS)₈],^{9c} but we cannot rule out the possibility that it is a mixture of U^{IV} and [UO₂]⁺. 1 shows a similar emission profile (Fig. S9–S11†). The emission lifetimes in solution are 0.46 μs and 0.40 μs for 1 and 2, respectively, shorter than the ca. 1 μs measured for the series [R₄N][UO₂(NCS)₅],¹¹ or the known [UO₂]⁺ complexes.¹⁸

As spectroscopic and structural evidence supports our [U^{IV}-U^V-U^{IV}][U^{VI}] formulation for 2, so it was of interest to examine the magnetic properties. The magnetic data of powdered single crystals of 2 are shown in Fig. 4 as μ_{eff} vs. T plots at 0.1 and 1.0 T, and M_m vs. B at 2.0 K (inset). At 300 K, the

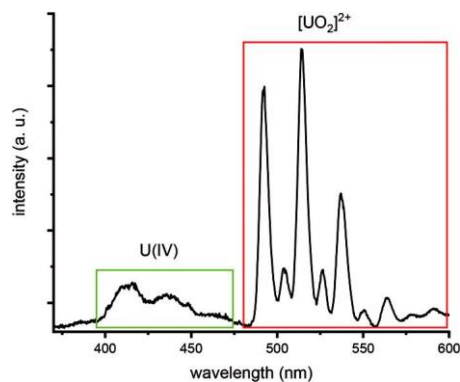


Fig. 3 Emission spectrum of 2 in the solid state at 77 K ($\lambda_{\text{ex}} = 330$ nm).

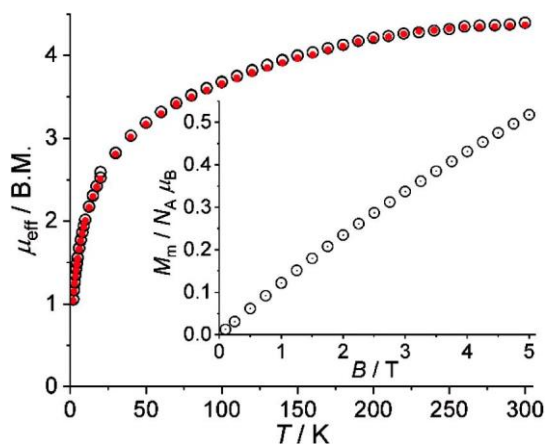


Fig. 4 Effective magnetic moment of 2 at 0.1 T (open black circles) and 1.0 T (red full dots); inset: molar magnetization at 2.0 K.

effective magnetic moment is $4.39\mu_{\text{B}}$ at 0.1 T and marginally smaller at 1.0 T ($4.37\mu_{\text{B}}$). Upon cooling, the effective moment gradually decreases with temperature, characterized by a sharp drop of μ_{eff} below 50 K. At 2.0 K, the moment reaches a value of 1.05 and $1.04\mu_{\text{B}}$ at 0.1 and 1.0 T, respectively. This marginal difference is also reflected by the shape of the molar magnetization. At this temperature, M_{m} is an almost linear function of the applied field up to 5.0 T, indicating a virtually constant magnetic susceptibility in this field range, which yields a value of $0.5N_{\text{A}}\mu_{\text{B}}$ at the highest field. Whilst it is difficult to delineate oxidation states based on the effective magnetic moment at room temperature, the shape of the magnetic response vs. temperature is more informative.^{3e} This is due to the wide range of μ_{eff} values for a single oxidation state that overlaps with the ranges of the other oxidation states. This general observation for actinides can be attributed to the similar energetic order of the relevant effects, namely electron–electron interrepulsion, spin–orbit coupling and ligand field effect. Summing the room temperature mean values of the U^{IV} and

U^{V} compounds reported in ref. 3e yields $\mu_{\text{eff}} = (2 \times 2.77^2 + 2.07^2)^{1/2} = 4.43\mu_{\text{B}}$, very close to the measured value for 2. This very good agreement alone should, however, not be used as

proof of the postulated $[\text{U}^{\text{IV}}-\text{U}^{\text{V}}-\text{U}^{\text{IV}}][\text{U}^{\text{VI}}]$ scenario due to the large variances of these mean values. Regarding the shape of the temperature dependence of μ_{eff} , U^{IV} compounds generally show a precipitous drop at temperatures below ca. 50 K, whilst U^{V} (or U^{III}) compounds tend to a more linear temperature dependence. A precipitous drop at 50 K is clearly evident from the data, supporting the hypothesis of a $\text{U}(\text{IV})$ ion. In addition, the mean value of μ_{eff} at 1.8 K is $1.67\mu_{\text{B}}$,^{3e} i.e. larger than the observed value for 2. While this may be solely due to the single-ion effects of each uranium site, this may also indicate the presence of relevant exchange interactions. Considering the small values of the molar magnetization combined with an almost linear shape, exchange coupling most likely is anti-ferromagnetic and weak. Moreover, the data does not fit to any model that does not contain a $\text{U}(\text{V})$ ion (Fig. S14†). Coupling in mixed-valent $\text{U}^{\text{IV/V}}$ using an aryloxo-substituted tacn ligand¹⁹ or in a pacman type²⁰ polypyrrolic $\text{U}^{\text{V}}-\text{U}^{\text{IV}}\text{Cp}_3$ were also observed to be weak. In contrast, CCIs in Np compounds can show strong exchange coupling, such as in the mixed valent $[\{\text{Np}^{\text{VI}}\text{O}_2\text{Cl}_2\}\{\text{Np}^{\text{V}}\text{O}_2\text{Cl}(\text{thf})_3\}_2]$,²¹ but more relevant to this work, $[\text{Np}^{\text{IV}}(\text{Np}^{\text{V}}\text{O}_2)_2(\text{SeO}_3)_3]$ does not.²² Thus, in addition to the spectroscopic and structural evidence, the magnetic data also support the proposed $[\text{U}^{\text{IV}}-\text{U}^{\text{V}}-\text{U}^{\text{IV}}][\text{U}^{\text{VI}}]$ structure of 2. Finally, it is worth noting that fully understanding the magnetic behaviour of a single actinide centre is still challenging,²³ so a quantitative explanation of the exchange interactions requires more sophisticated models to be developed.

To explore the bonding in 2 we utilised DFT calculations. A model of the cationic component of 2, where the DMF solvent molecules are cut down to H_2NCO , was extracted from the crystal structure, with H atoms placed at idealised bond lengths from neutron diffraction data and all other atoms fixed at crystallographic coordinates. DFT calculations used RI-BP86 functional and a basis set consisting of Lan12DZ 78-electron ECP/basis on U and def2-TZVP (-f) on light atoms. Efforts to use smaller core ECPs failed due to SCF convergence problems. Three possible spin states were tested, predicting that sextet is preferred by 0.37 and 0.56 eV over doublet and quartet, respectively, consistent with parallel alignment of spins from all U centres in $[\text{U}^{\text{IV}}-\text{U}^{\text{V}}-\text{U}^{\text{IV}}]$. A plot of DFT spin density from sextet state is shown in Fig. 5, lending further

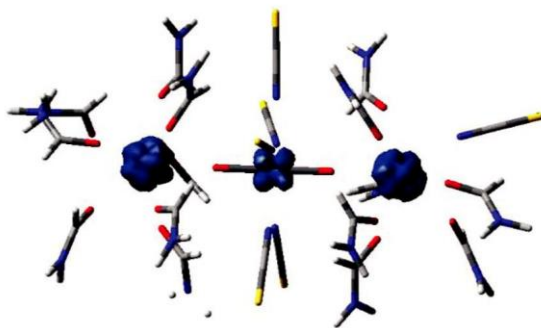


Fig. 5 Plot of the DFT spin density from sextet state of a model of 2.

support to the alignment of the central U as U^V. Mayer bond orders from the sextet calculation support the presence of CCIs in the central cation: orders of 1.44 and 1.45 are found for U2–O39 and U2–O45, respectively, compared to 0.47 for U1–O39 and U3–O45. For comparison, bond orders of ca. 0.38 and 0.48 are observed for U–ODMF and U–N, respectively. Atoms-in-Molecules (AIM) analysis supports this assignment: ρ_{BCP} is 0.20 au in U2–O39 and U2–O45, but just 0.07 au in U1–O39 and U3–O45. All U–O bonds are closed shell, with $\nabla^2\rho_{\text{BCP}}$ values of +0.33 au for U2–O39 and U2–O45 and +0.27 au for U1–O39 and U3–O45, although negative energy densities, HBCP, of –0.13 au for central UVO bonds indicate significant covalent character. This study gives some insight into the oxidation of U^{IV} compounds. Clearly [UO₂]⁺ is able to be trapped using coordinating solvents but how general or reproducible this method could be is not obvious from our study; we have previously characterised Cs₃[UO₂(NCS)₅] from the oxidation of Cs₄[U(NCS)₈] in the solid state over some months,^{9c} so presumably the isolation of 1 and 2 reflects their solubility in different solvents. Controlled hydrolysis of UCl₄ with benzoate have shown that clusters of varying size can form but are time dependent.²⁴ Some examples have been reported of mixed-valent uranium compounds,²⁵ but these are mainly from hydrothermal syntheses and concomitant reduction of [UO₂]²⁺ precursors. These observations suggest further investigation on oxidation reactions of U^{IV} are war-ranted and likely dependent upon the supporting ligands. In summary, we have isolated two mixed-valent species that offer a snapshot on the oxidation of U^{IV} to U^{VI}. Spectroscopic, mag-netic and computational investigations confirm that 2 contain uranium in three different oxidation states simultaneously. The magnetic data are compatible with the proposed oxidation states and indicate that coupling between the U^V and U^{IV} centres is very weak.

Conflicts of interest

There are no conflicts to declare.

Notes and references

- Selected recent reviews: (a) T. W. Hayton and N. Kaltsoyannis, *Organometallic Actinide Complexes with Novel Oxidation States and Ligand Types*, in *Experimental and theoretical approaches to actinide chemistry: from fundamental systems to practical applications*, ed. J. K. Gibson and W. A. de Jong, John Wiley & Sons Inc., 2018; (b) P. L. Arnold, M. S. Dutkiewicz and O. Walter, *Chem. Rev.*, 2017, 117, 11460; (c) C. D. Tutson and A. E. V. Gorden, *Coord. Chem. Rev.*, 2017, 333, 27; (d) S. T. Liddle, *Angew. Chem., Int. Ed.*, 2015, 54, 8604; (e) M. B. Jones and A. J. Gaunt, *Chem. Rev.*, 2013, 113, 1137.
- (a) M. R. MacDonald, M. E. Fieser, J. E. Bates, J. W. Ziller, F. Furche and W. J. Evans, *J. Am. Chem. Soc.*, 2013, 135, 13310; (b) H. S. La Pierre, A. Scheurer, F. W. Heinemann, W. Hieringer and K. Meyer, *Angew. Chem., Int. Ed.*, 2014, 53, 7158.
- (a) N. Magnani and R. Caciuffo, *Inorganics*, 2018, 6, 26; (b) S. G. McAdams, A.-M. Ariciu, A. K. Kostopoulos, J. P. S. Walsh and F. Tuna, *Coord. Chem. Rev.*, 2017, 346, 216; (c) K. R. Meihaus and J. D. Long, *Dalton Trans.*, 2015, 44, 2517; (d) S. T. Liddle and J. van Slageren, *Chem. Soc. Rev.*, 2015, 44, 6655; (e) D. R. Kindra and W. J. Evans, *Chem. Rev.*, 2014, 114, 8865.
- (a) D. M. King, P. A. Cleaves, A. J. Wooles, B. M. Gardner, N. F. Chilton, F. Tuna, W. Lewis, E. J. L. McInnes and S. T. Liddle, *Nat. Commun.*, 2016, 7, 13773; (b) D. M. King, F. Tuna, J. McMaster, W. Lewis, A. J. Blake, E. J. L. McInnes and S. T. Liddle, *Angew. Chem., Int. Ed.*, 2013, 52, 4921.
- Recent examples: (a) V. Mougél, L. Chatelain, J. Pécaut, R. Caciuffo, E. Colineau, J.-C. Griveau and M. Mazzanti, *Nat. Chem.*, 2012, 4, 1011; (b) L. Chatelain, V. Mougél, J. Pécaut and M. Mazzanti, *Chem. Sci.*, 2012, 3, 1075; (c) L. Chatelain, F. Tuna, J. Pécaut and M. Mazzanti, *Chem. Commun.*, 2015, 51, 11309.
- See e.g.: (a) P. L. Arnold, E. Hollis, G. S. Nichol, J. B. Love, J.-C. Griveau, R. Caciuffo, N. Magnani, L. Maron, L. Castro, A. Yahia, S. O. Odoh and G. Schreckenbach, *J. Am. Chem. Soc.*, 2013, 135, 3841; (b) P. L. Arnold, B. E. Cowie, M. Suvova, M. Zegke, N. Magnani, E. Colineau, J.-C. Griveau, R. Caciuffo and J. B. Love, *Angew. Chem., Int. Ed.*, 2017, 56, 10775.
- B. Vlasisavljevich, P. Miró, D. Ma, G. E. Sigmon, P. C. Burns, C. J. Cramer and L. Gagliardi, *Chem. – Eur. J.*, 2013, 19, 2937.
- H. Steele and R. J. Taylor, *Inorg. Chem.*, 2007, 46, 6311.
- (a) E. Hashem, A. N. Swinburne, C. Schulzke, R. C. Evans, J. A. Platts, A. Kerridge, L. S. Natrajan and R. J. Baker, *RSC Adv.*, 2013, 3, 4350; (b) E. Hashem, G. Lorusso, M. Evangelisti, T. McCabe, C. Schulzke, J. A. Platts and R. J. Baker, *Dalton Trans.*, 2013, 42, 14677; (c) E. Hashem, J. A. Platts, F. Hartl, G. Lorusso, M. Evangelisti, C. Schulzke and R. J. Baker, *Inorg. Chem.*, 2014, 53, 8624.
- S. Biswas, S. Ma, S. Nuzzo, B. Twamley, A. T. Russel, J. A. Platts, F. Hartl and R. J. Baker, *Inorg. Chem.*, 2017, 56, 14426.
- S. Nuzzo, B. Twamley, J. A. Platts and R. J. Baker, *Inorg. Chem.*, 2018, 57, 3699.
- M. Nyman, M. A. Rodriguez and C. F. Campana, *Inorg. Chem.*, 2010, 49, 7748.
- R. D. Shannon, *Acta Crystallogr., Sect. A: Cryst. Phys., Diffr., Theor. Gen. Crystallogr.*, 1976, 32, 751.
- SHAPE Program for the Stereochemical Analysis of Molecular Fragments by Means of Continuous Shape Measures and Associated Tools, v2.1, 2013.
- J.-C. Berthet, P. Thuéry and M. Ephritikhine, *Polyhedron*, 2006, 25, 1700.
- J.-C. Berthet, P. Thuéry and M. Ephritikhine, *Inorg. Chem.*, 2005, 44, 1142.
- L. S. Natrajan, *Coord. Chem. Rev.*, 2012, 256, 1583.

- 18 (a) K. Grossmann, T. Arnold, A. Ikeda-Ohno, R. Steudtner, G. Geipel and G. Bernhard, *Spectrochim. Acta, Part A*, 2009, 72, 449; (b) R. Steudtner, T. Arnold, K. Großmann, G. Geipel and V. Brendler, *Inorg. Chem. Commun.*, 2006, 9, 939.
- 19 A.-C. Schmidt, F. W. Heinemann, W. W. Lukens, Jr. and K. Meyer, *J. Am. Chem. Soc.*, 2014, 136, 11980.
- 20 P. L. Arnold, M. S. Dutkiewicz, M. Zegke, O. Walter, C. Apostolidis, E. Hollis, A.-F. Pécharman, N. Magnani, J.-C. Griveau, E. Colineau, R. Caciuffo, X. Zhang, G. Schreckenbach and J. B. Love, *Angew. Chem., Int. Ed.*, 2016, 55, 12797.
- 21 N. Magnani, E. Colineau, R. Eloirdi, J.-C. Griveau, R. Caciuffo, S. M. Cornet, I. May, C. A. Sharrad, D. Collison and R. E. P. Winpenny, *Phys. Rev. Lett.*, 2010, 104, 197202.
- 22 P. M. Almond, R. E. Sykora, S. Skanthakumar, L. Soderholm and T. E. Albrecht-Schmitt, *Inorg. Chem.*, 2004, 43, 958.
- 23 J. van Leusen, M. Speldrich, H. Schilder and P. Kögerler, *Coord. Chem. Rev.*, 2015, 289–290, 137.
- 24 L. Chatelain, R. Faizova, F. Fadaei-Tirani, J. Pécaut and M. Mazzanti, *Angew. Chem., Int. Ed.*, 2019, 58, 3021.
- 25 Selected examples: (a) L. Chen, J. Diwu, D. Gui, Y. Wang, Z. Weng, Z. Chai, T. E. Albrecht-Schmitt and S. Wang, *Inorg. Chem.*, 2017, 56, 6952; (b) L. Chatelain, S. White, R. Scopelliti and M. Mazzanti, *Angew. Chem., Int. Ed.*, 2016, 55, 14325; (c) L. Chen, T. Zheng, S. Bao, L. Zhang, H.-K. Liu, L. Zheng, J. Wang, Y. Wang, J. Diwu, Z. Chai, T. E. Albrecht-Schmitt and S. Wang, *Chem. – Eur. J.*, 2016, 22, 11954.